RGS small window mode

A.M.T. Pollock & M. Diaz Trigo on behalf of the RGS IDT

11 June 2010

1 The brightest X-ray sources in modern astrophysics

While rapid advances in detector and mirror technology have allowed X-rays to be observed from fainter and fainter sources probing, for example, the early Universe or the far reaches of luminosity distributions, there are significant scientific problems that can only feasibly be addressed by using the brightest X-ray sources. In this document, we show that with use of the new small window mode, the RGS offers opportunities for advances in these studies by alleviating some of the instrumental difficulties of observing bright sources, notably that of pile-up. The quantitative study described below shows that pile-up occurs in the RGS in normal spectroscopy mode at flux levels per CCD typical of the brightest few dozen X-ray sources in the sky at any one time, in conditions not dissimilar to those which encourage the use of EPIC timing modes. We recommend that use of the RGS small window mode should be considered by observers or during proposal enhancement for a wide range of observations. All operational issues are in place and the mode is ready to be offered to the community in AO10.

Three scientific problems are of particular current relevance to XMM :

- emission lines produced in the strong gravity near black holes and neutron stars;
- X-ray absorption by warm circumsource material;
- X-ray absorption in the interstellar and intergalactic medium.

1.1 Probing strong gravity

Relativistically-broadened emission lines are thought to be present in the Fe-K band accessible to EPIC of many galactic and extragalactic X-ray spectra and claims have also been made of similar broad features in the RGS band below 2 keV, due perhaps to the equivalent Fe-L shell emission, although nearly all of this work has been confined to EPIC.

1.2 Photoionized winds and atmospheres

Winds, jets and mass outflows in general are ubiquitous in accretion-powered sources from YSOs to X-ray binaries (XRBs) and supermassive black holes (SMBHs), transporting energy and angular momentum away and thus playing a key role in processes as diverse as stellar evolution or AGN feedback. The source of the wind is unknown. The driving forces could be of thermal, radiative or magnetic origin and might differ from source to source. The last decade has seen many discoveries of hot atmospheres and winds in XRBs. These systems bridge the gap between YSOs and SMBHs and

may hold the answers to the driving mechanisms. XRBs can show either general relativistic effects, when black holes are involved, or the effects of strong magnetism in neutron stars, allowing the role of the compact object to be isolated in driving the winds. In particular, the presence of highly-ionized plasma around compact objects has been observed close to the disc in all high-inclination XRBs. Such plasma has also been detected as outflowing winds in BHs and in one NS XRB. As the amount of mass expelled could vary considerably in different circumstances, this has important consequences for the impact of the winds on XRB disc structure, for example, and in the close environments more generally. It is crucial to quantify these mass outflows.

1.3 Mapping the ISM

One of the paramount questions in physics concerns the origin and distribution of the matter currently in the Universe as determined by the history of nucleosynthesis and stellar evolution since the big bang. High-resolution absorption X-ray spectroscopy is a powerful means to probe interstellar and intergalactic media through the imprint of their lines and edges on the strong continuum of a distant X-ray source. Elemental abundances, ionization structure, and velocity dispersion are all open to the current grating spectrometers aboard XMM-Newton and Chandra. High-resolution spectra of XRBs show absorption by three different phases of the ISM in lines of equivalent widths between about 1 and 15 mÅ and column densities up to $10^{18}\mathrm{cm}^{-2}$. In contrast to traditional UV studies of the local ISM, the brightness and kpc distances of XRBs allows scans of the entire Galactic plane. The combination of the RGS's waveband and its higher sensitivity than any of the Chandra instruments should make it the instrument of choice for such work.

1.4 Pile-up in observations of bright X-ray sources with XMM-Newton

Observations of bright X-ray sources are regularly performed with *XMM-Newton* for precisely the study of strong gravity, high excitation plasma or absorption spectroscopy although the high count rates pose instrumental challenges. Pile-up is a familiar problem with CCD detectors and occurs when two or more events coincide in space and time in the same integration element. In the non-dispersive EPIC instruments aboard *XMM-Newton*, bright-source observations involve either the *a priori* use of timing modes, in which spatial information is discarded in favour of high time resolution, or *a posteriori* imaging-mode analysis combining event pattern selection and rejection of central regions of the PSF in order to mitigate or eliminate the effects of pile-up. The proper scientific exploitation of XMM data undoubtedly requires taking full advantage of the opportunities offered by the accompanying RGS to illuminate the underlying physics. Naturally, this requires an assessment of the performance of the RGS in the observation of bright sources.

2 Pile-up in the RGS

Very bright sources also suffer pile-up in the dispersed spectra delivered by the RGS [1] where the most obvious effect is the spurious migration of events from 1st to 2nd order. As the RGS calibration ensures the close agreement of the 1st and 2nd order spectra in physical units in sources where pile-up is not significant, the comparison of these spectra provides a test for pile-up in RGS data. Fig, 1, compares smoothed versions of the 1st and 2nd order fluxed spectra produced by `rgsproc` in the calibrated waveband of a set of suitably bright point sources, allowing the following conclusions to be drawn:

- The differences between the 1st and 2nd order spectra increase with source brightness
- EXO0748-676's 1st and 2nd order spectra agree well
- Differences in the other spectra are most probably due to pile-up losses
- The brightest source, Cyg X-2, shows large differences over a wide range of its continuum
- Pile-up in Capella is obvious in the brightest lines

When 1st-order pile-up losses are significant, the corresponding spurious 2nd order events should appear at $\lambda/2$. For heavily-absorbed LMXRBs, this lies in the uncalibrated region below 6Å. Fig. 2, which extends to uncalibrated shorter wavelengths, shows 2nd-order excesses where expected.

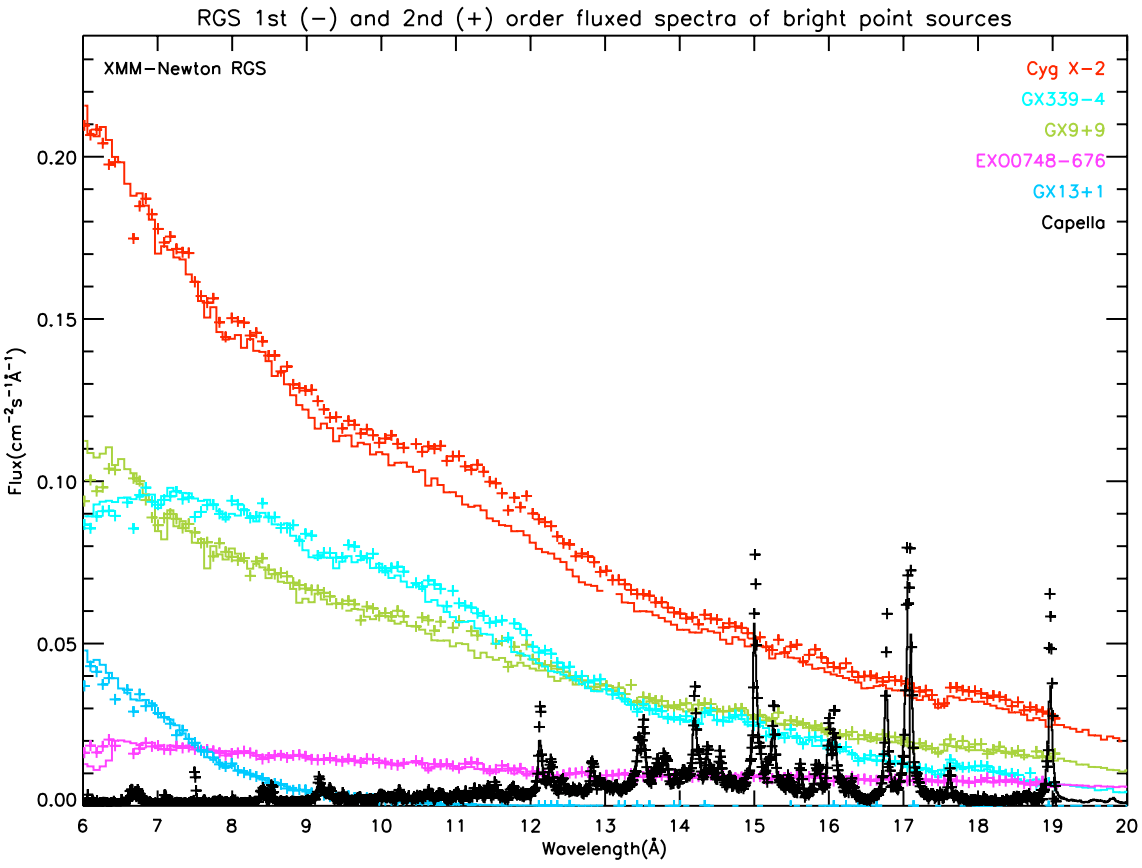

Figure 1: 1st and 2nd order fluxed spectra of a selection of bright sources between 6 and 20 Å.

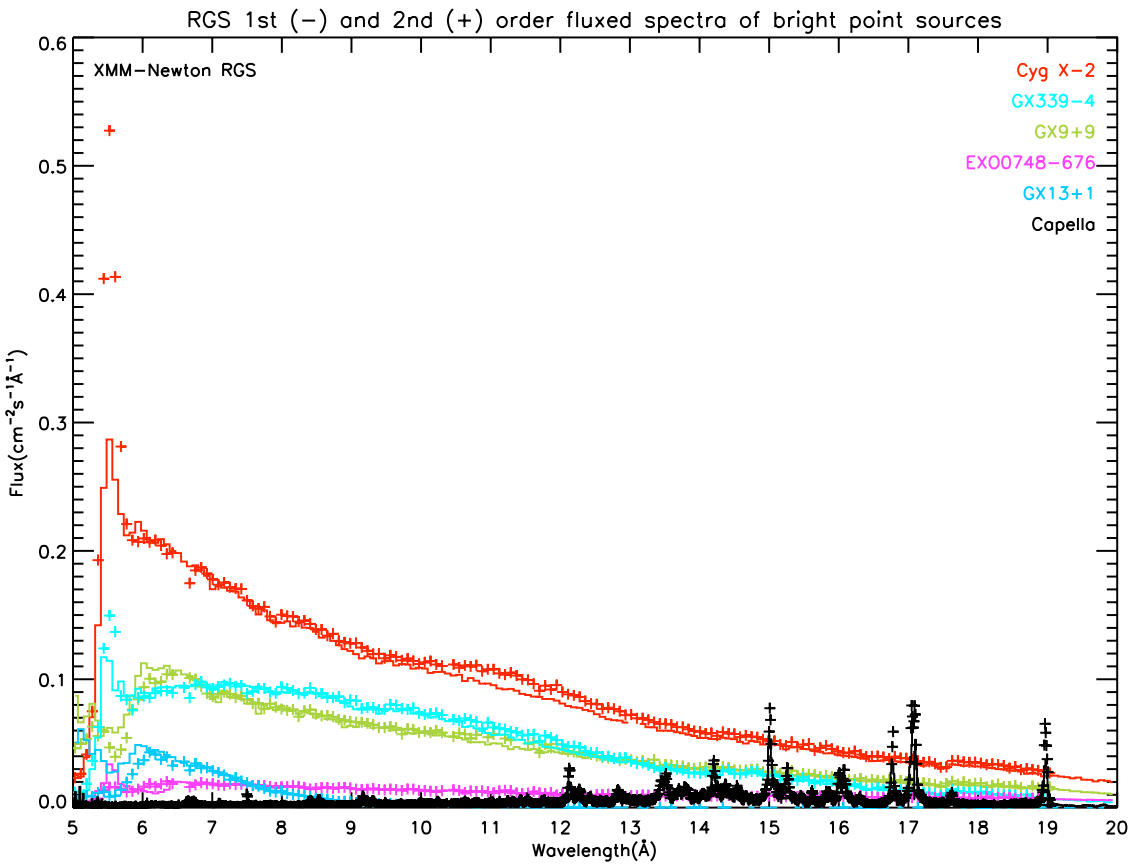

Figure 2: The spectra of Fig. 1 extended shortwards to 5 Å where the RGS is not well-calibrated but piled-up events are expected.

3 The proposed RGS small-window mode

A straightforward method of dealing with pileup is to reduce the intervals in which data are accumulated. RGS data from an on-axis point source cover about one third of the RGS detectors in the cross-dispersion direction while simultaneous background estimates are usually made using off-axis data. For the bright point sources mostly affected by pile-up, the RGS background is often negligible. Therefore, new clock sequences have been generated for RGS1 and RGS2 to read only the central 32 of 128 CHIPY cross-dipsersion rows in order to preserve most of the source signal in shorter integration times at the expense of the background. The new mode was initially successfully tested on the extended Crab nebula and subsequently the test was also performed on Cyg X-2, a point source chosen for the combination of its reliable brightness and modest interstellar absorption. Cyg X-2 was the second brightest source in the ROSAT All-Sky Survey slew catalogue and also accounted for 14 of the 15 brightest entries in the pointed ROSPSPC catalogue.

4 The 1726_0561180501 Cyg X-2 RGS small window test

Compared to the mean `rgslccorr` count rates in earlier observations of 159 cts/s in 0455_0111360101 and 134 cts/s in 1010_0303280101 in spectroscopy mode, Cyg X-2 was fainter at 93 cts/s. The allocated observation time of 25ks was split into 4 pairs of exposures as follows

RGS1			RGS2		
ExpID	T(s)	CCDs	ExpID	T(s)	CCDs
8-CCD Spec+Q					
S002	5863	98 654321	S004	5854	98765 321
8-CCD small window mode					
S003	7872	98 654321	S005	7874	98765 321
4-CCD small window mode					
S008	5702	98 65	S010	5704	9876
2-CCD small window mode					
S009	5702	98	S011	5704	98

in order to compare the behaviour of the instrument in normal spectroscopy mode with the small window mode with 8, 4 and 2 CCDs with correspondingly shorter integration times. The EPIC-pn instrument was operated continuously in Burst Mode to provide a simultaneous count rate monitor. The test went smoothly in operational terms and was followed within a few days by delivery of the ODF. The RGS data were immediately processed to completion by the current public version of `rgsproc`, making spectra and response matrices available for further analysis which consisted of the following steps:

- Inspection of raw ODF data
- Results of `rgsproc`
- Generation of light curves with `epproc`, `xmmselect`, `epiclccorr` and `rgslccorr`.
- Inspection of RGS spectra

4.1 ODF RGS data

Inspection of individual CCD data files and the associated auxiliary data allowed the derivation of statistics concerning the raw data shown in Table 1. Of note among the statistics are the mean frame times which are reduced from 4.6s and 9.0s for RGS1 and RGS2 respectively in normal 8-CCD spectroscopy mode, successively to 1.2s and 2.3s in the 8-CCD small window; 0.6s and 1.1s with 4 CCDs; and 0.3s and 0.57s with 2 CCDs. The numbers of empty frames, those that contain no events, are consistent with Poisson statistics.

	CCD	dT(s)	frames	empty	missing	NLOSTEVT	Counts	Cts/Frame
8-CCD Spec+Q								
R1S00201SPE.FIT	1	4.5952	1271	4	0	0/0	21526	16.9
R1S00202SPE.FIT	2	4.5952	1271	0	0	0/0	28072	22.1
R1S00203SPE.FIT	3	4.5952	1271	0	0	0/0	47971	37.7
R1S00204SPE.FIT	4	4.5952	1271	1	0	0/0	71584	56.3
R1S00205SPE.FIT	5	4.5952	1271	1	0	0/0	94326	74.2
R1S00206SPE.FIT	6	4.5952	1270	36	0	0/0	122911	96.8
R1S00208SPE.FIT	8	4.5952	1270	107	0	0/0	127829	100.6
R1S00209SPE.FIT	9	4.5952	1270	0	0	0/0	69064	54.4
R2S00401SPE.FIT	1	9.0433	640	4	0	0/0	22782	35.6
R2S00402SPE.FIT	2	9.0433	640	0	0	0/0	29899	46.7
R2S00403SPE.FIT	3	9.0433	640	14	0	0/0	55593	86.8
R2S00405SPE.FIT	5	9.0433	639	60	0	0/0	87375	136.7
R2S00406SPE.FIT	6	9.0433	639	67	0	0/0	38940	61.0
R2S00407SPE.FIT	7	9.0433	639	24	0	0/0	8591	13.5
R2S00408SPE.FIT	8	9.0433	639	3	0	0/0	11406	17.9
R2S00409SPE.FIT	9	9.0433	639	15	0	0/0	41815	65.4
8-CCD Small Window								
R1S00301SPE.FIT	1	1.2158	6416	473	27	0/0	17421	2.7
R1S00302SPE.FIT	2	1.2160	6415	86	28	51/1	28348	4.4
R1S00303SPE.FIT	3	1.2160	6415	1	28	0/0	54652	8.5
R1S00304SPE.FIT	4	1.2156	6417	1	26	0/0	81845	12.7
R1S00305SPE.FIT	5	1.2156	6417	0	26	2309/1	109163	16.9
R1S00306SPE.FIT	6	1.2156	6417	1	26	0/0	144919	22.5
R1S00308SPE.FIT	8	1.2158	6416	1	27	0/0	156667	24.3
R1S00309SPE.FIT	9	1.2158	6415	0	27	1690/1	78627	12.2
R2S00501SPE.FIT	1	2.2713	3435	7	14	0/0	20521	5.9
R2S00502SPE.FIT	2	2.2713	3434	1	14	0/0	34000	9.8
R2S00503SPE.FIT	3	2.2713	3434	1	14	2092/1	70633	20.5
R2S00505SPE.FIT	5	2.2713	3434	0	14	1014/1	118895	34.5
R2S00506SPE.FIT	6	2.2720	3433	0	15	1843/1	155513	45.1
R2S00507SPE.FIT	7	2.2720	3433	1	15	0/0	153	50.1
R2S00508SPE.FIT	8	2.2720	3433	1	15	0/0	147352	42.7
R2S00509SPE.FIT	9	2.2713	3434	1	14	3263/1	51580	15.0
4-CCD Small Window								
R1S00805SPE.FIT	5	0.6053	8259	4	0	20/1	70838	8.5
R1S00806SPE.FIT	6	0.6053	8259	2	0	2339/1	93575	11.3
R1S00808SPE.FIT	8	0.6053	8259	3	0	0/0	101645	12.3
R1S00809SPE.FIT	9	0.6053	8259	12	0	0/0	50962	6.2
R2S01006SPE.FIT	6	1.1310	4421	0	0	0/0	101591	23.0
R2S01007SPE.FIT	7	1.1310	4421	0	0	1577/1	113844	25.8
R2S01008SPE.FIT	8	1.1310	4421	1	0	0/0	98037	22.2
R2S01009SPE.FIT	9	1.1310	4421	3	0	0/0	33585	7.6
2-CCD Small Window								
R1S00908SPE.FIT	8	0.3027	16498	57	0	850/1	96166	5.8
R1S00909SPE.FIT	9	0.3027	16497	878	0	1970/1	49636	3.0
R2S01108SPE.FIT	8	0.5654	8843	1	0	761/1	94685	10.7
R2S01109SPE.FIT	9	0.5654	8842	209	0	2789/1	32655	3.7

4.2 Results of `rgsproc`

As mentioned above, the SAS task `rgsproc` ran to completion. Inspection of the small-window mode RGS1 and RGS2 calibrated event files showed the following:

- RGS1 $50 \leq$ `CHIPY` ≤ 79; source centred at `CHIPY` ≈ 60.6
- RGS2 $50 \leq$ `CHIPY` ≤ 79; source centred at `CHIPY` ≈ 64.8

As expected, the source was well centred in RGS2 and slightly asymmetrically placed in RGS1, although without any significant consequences. There was no sign of the excess counts at the `CHIPY` edges of the small-window aperture seen in some of the earlier operational tests.

4.3 Background issues

Changes to the operational database have ensured that the CCD9 radiation monitor used to protect the EPIC instruments is still operational in small window mode.

As far as the SAS is concerned, the absence in the small-window exposures of the off-axis data usually used to calculate simultaneous estimates of the RGS background caused some benign problems with the set of BGSPEC files containing null values. Although it could be argued that this is an accurate description of the circumstances, a more elegant solution is required and the subject of a SAS SCR. As the cross-dispersion distribution of a point source is well-known, it is conceivable that future model fitting may be able to provide background estimates anyway.

The synthetic backgrounds produced by `rgsbkgmodel` were incorrect, reflecting the lowest-rate background templates rather than unknown values. Radiation parameters used operationally for EPIC protection are available to the SAS in HK data and, following a comparison exercise of these values with normal particle background parameters to be completed by the end of 2010, it is expected that they will be able to be used instead to drive the RGS synthetic background model generation.

4.4 Light curve analysis

EPIC-pn was operating in burst mode throughout the test, monitoring the variations of Cyg X-2. Fig. 3 shows a comparison between RGS and EPIC-pn light curves generated from the calibrated event files with `epiclccorr` and `rgslccorr`. The effects of using the small window mode are clear:

- 50% increase in count rate for the full set of CCDs between Spec+Q and 8-CCD SW;
- better correlation with EPIC-pn variations;
- good agreement between 4CCD and 2CCD SW data from CCDs 8 and 9.

The few percent difference between the CCDs 8 and 9 light curve selected from the 8-CCD SW is probably due to residual pileup. This should be tested through separate analysis of RGS1 and RGS2.

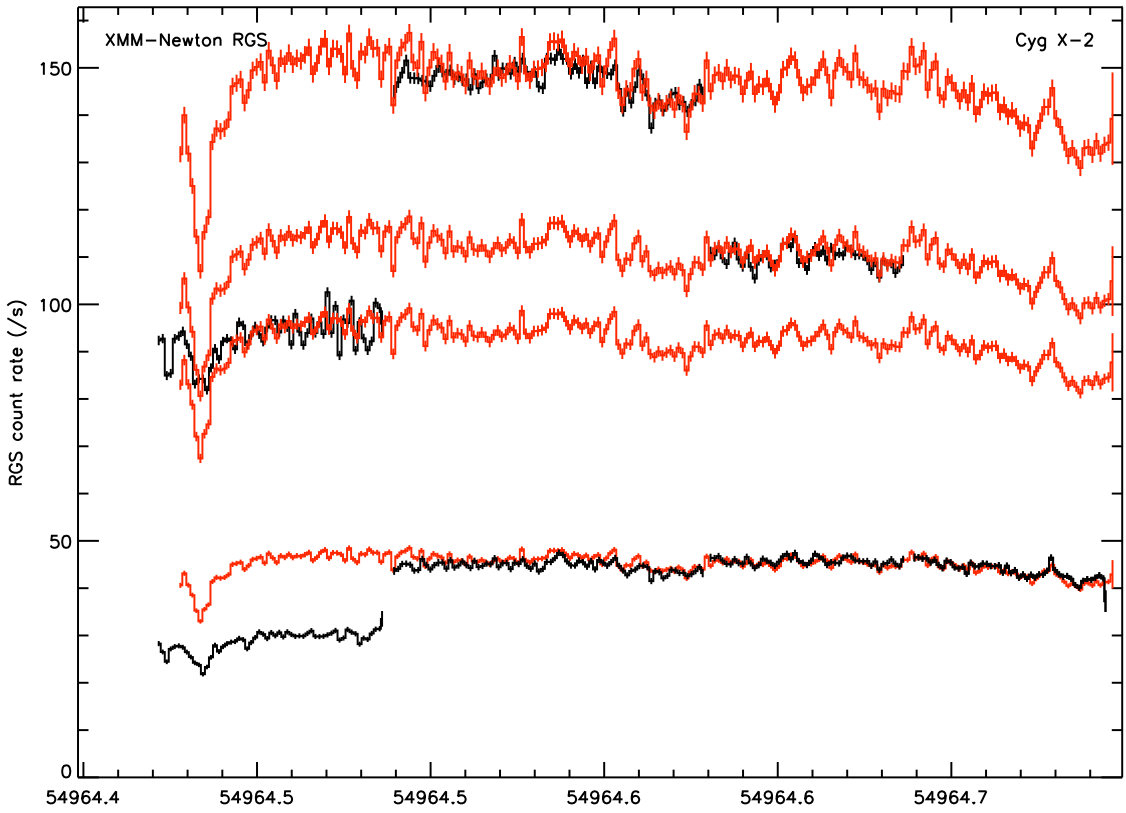

Figure 3: Combined RGS1+RGS2 light curves generated with `rgslccorr` in black compared with the EPIC-pn burst mode light curve below 2 keV in red that appears 4 times on the plot conveniently renormalised. No background corrections were applied. The transitions in the RGS light curves are clear between the initial 8-CCD Spec+Q exposures and the subsequent 8-CCD, 4-CCD and 2-CCD small window exposures. The lowest black RGS curve shows CCDs 8 and 9 throughout.

4.5 RGS spectra

Fig. 4 shows the 1st and 2nd order fluxed spectra of Cyg X-2 during the test, calculated separately for RGS1 and RGS2. As expected, the normal spectroscopy mode spectra are poor, especially for the longer readout times of RGS2. By contrast, the small window spectra are smooth. There is one concern about the RGS1 2nd order data in the wavelength range near 11Å affected by the absence of RGS1 CCD7. There is a 10-15% discrepancy and this is confirmed by Xspec analysis. A possible explanation is a problem with the RGS1 2nd order correction although Fig. 1 showed no obvious similar problems for not such bright sources as Cyg X-2.

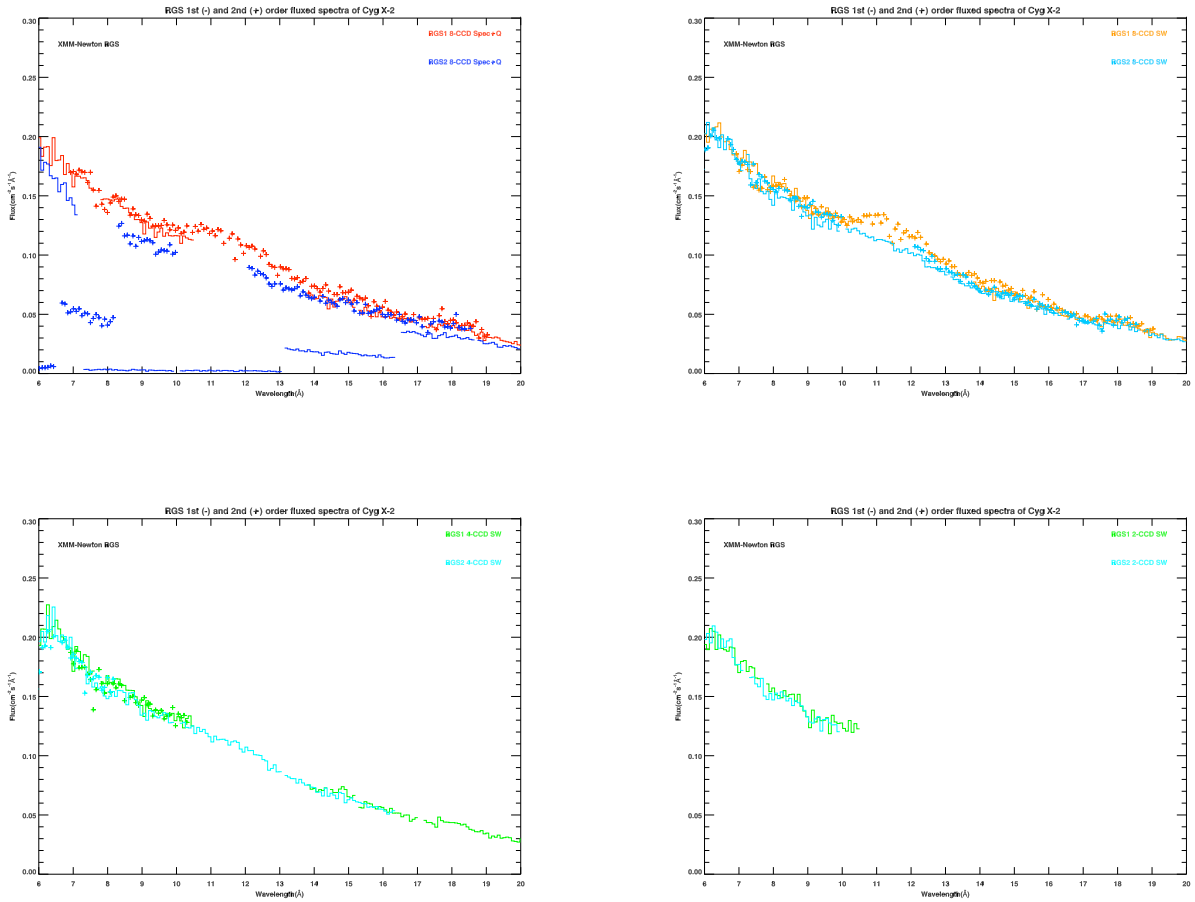

Figure 4: 1st and 2nd order fluxed spectra of RGS1 and RGS2 separately during the four separate parts of the small window test on Cyg X-2 namely 8-CCD Spec+Q (top left); 8-CCD small window (top right); 4-CCD small window (bottom left); and 2-CCD small window (bottom right).

5 A quantitative survey of pile-up in the RGS

The comparison of 1st and 2nd order RGS spectra described above is a qualitative procedure similar in scope to the SAS task `epatplot` used to assess EPIC pile-up. We have performed a more quantitative study starting from the simplest expectations of Poisson statistics. The key parameter that determines the level pile-up in an instrument element is μ, the expected count rate per integration time or frame. In a single element, the probability of detecting n events is given by the Poisson formula :

$$\begin{aligned} P(n|\mu) &= e^{-\mu}\mu^n/n! \\ P(0|\mu) &= e^{-\mu} \\ P(1|\mu) &= e^{-\mu} \times (\mu/1) \\ P(2|\mu) &= e^{-\mu} \times (\mu/1) \times (\mu/2) \\ P(3|\mu) &= e^{-\mu} \times (\mu/1) \times (\mu/2) \times (\mu/3) \end{aligned}$$

and so on. Pile-up occurs for $n \geq 2$. For $\mu \ll 1.$, the level of pile-up in these simple circumstances is about $P(2|\mu)/P(1|\mu) = \mu/2$. The level of pile-up in a multi-pixel instrument will be larger than this because of events occuring simultaneously in adjacent pixels, so-called pattern pile-up, and we have taken μ, the count rate per pixel per frame, as a proxy for pile-up in the RGS. The analysis of Capella described below justifies this use of μ. Accordingly, a pixel with a frame count rate of μ cts per frame suffers pile-up at a level of $\mu/times100\%$. We have considered RGS pixels with $\mu > 0.01$ cts per pixel per frame, corresponding to 1% pile-up.

5.1 Source sample

Data of the following sources were considered :

Capella

Mkn421

Cyg X-1

Cyg X-2

EXO0748-676

4U1636-536

4U1735-44

4U1820-30

GX339-4

GX349+2

GX9+9

GX13+1

SAX1808.4-3658

GROJ1655-40

Ser X-1

XTEJ1650-500

Capella is the only source in the sample whose spectrum shows strong contrasts between nearby pixels caused by strong emission line spectrum above a weak or absent continuum.

5.2 Analysis procedure

Code written in IDL performed the following steps on the unfiltered merged RGS event files produced by rgsproc :

```
foreach unfilteredEventFile {
     foreach CCD {
         count the number of frames
         accumulate image in CHIPX,CHIPY coordinates
         calculate mean count rate per frame per pixel, mu
         eliminate hot pixels
         identify brightest pixel to use as pile-up proxy
         foreach pixel {
             accumulate PI histogram
             fit PI histogram with energy-dependent redistribution derived from CCF
             record best-fit parameters {
                 gain
                 background counts
                 1st order counts
                 2nd order counts
             }
         }
         accumulate simultaneous rgsfluxer data
    }
    accumulate simultaneous EPIC-pn data
}
```

5.3 Pile-up in the RGS spectrum of Capella

The strong emission lines in Capella give the opportunity to make a reliable quantitative assessment of the pile-up fraction. Fig. 5 shows 1st and 2nd order data from an RGS2 single-node readout observation of Capella. The top panel shows 1st and 2nd order ($\times 10$) counts on CCDs 5 and 6. The 2nd order data are a mixture of genuine 2nd order $\lambda/2$ events and 1st order pile-up migrations. The middle panel compares the same red 2nd order data with the 1st order ($\times 0.3$) data at the same wavelengths. The effects of pile-up are obvious. The pile-up fraction estimated at the positions of 4 bright lines are shown by the black stars in the lower panel along with the frame count rates for all pixels above the 0.01 threshold, which naturally cluster around the strong lines. Although systematically too low, the maximum pixel count rates give estimates of the pile-up fraction good to about 20%.

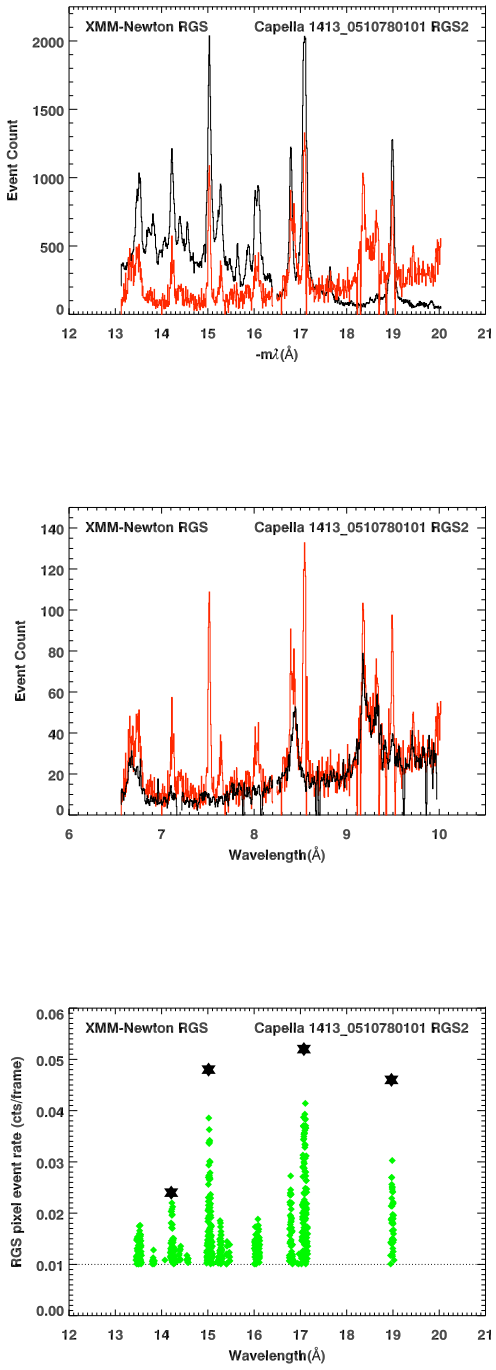

Figure 5: Effects of pile-up in an RGS2 single-node observation of Capella. The top panel shows the counts from 1st order (black) and 2nd order (red $\times 10$) from CCDs 5 and 6 on an $-m\lambda$ scale. A fraction of events from all the strong lines has migrated from 1st to 2nd order. The middle panel shows the same 2nd order events (red $\times 1$) against wavelength compared with the corresponding 1st order events (black $\times 0.3$). These two sets of data allow a robust and direct estimate of the pile-up fraction. The bottom panel compares these estimates at the peak of some of the strong lines with the pixel frame rates of all pixels with $\mu \geq 0.01$, showing the maximum pixel count rate gives quite a good estimate of the pile-up fraction.

5.4 Pile-up in RGS spectra

The maximum pixel count rates per frame, which the Capella analysis above shows is a good estimate of the pile-up fraction, have been calculated for CCDs 2-9 in about 100 RGS1 and RGS2 spectra of the sample of bright sources. CCD1 was excluded because of problems caused by fixed-pattern noise. Many other auxiliary data have been gathered in order to help interpret the pile-up fraction estimated in this way. Two instructive plots are shown in Figs. 6 and 7 in order to be able to understand the general conditions under which pile-up occurs in the RGS and the overall extent of damage to the spectrum.

5.4.1 Dependence of RGS pile-up on RGS CCD count rate

Fig. 6 shows that the pile-up fraction increases steadily with CCD count rate. Some of the scatter is caused by the higher pile-up fraction in the relatively small amount of RGS2 single-node data. For the relatively smooth continuum sources, including Mkn421, pile-up is below 1% for CCD count rates below about 20 cts/frame, equal to about 4 cts/s in double-node readout and 2 cts/s in single-node readout. Mkn421 is usually piled-up by a few percent in RGS2 single-node observations. The success of the RGS Small Window test for reducing the frame count rate for Cyg X-2 is clear. The high contrast of the line-rich Capella spectrum, on the other hand, causes pile-up to become significant at CCD count rates about a factor 4 lower.

The question arises now of how to devise a practical count rate threshold for guidance about RGS pile-up during proposal planning and enhancement for the smooth continuum spectra that form the majority of bright X-ray sources. As it is smaller than typical calibration uncertainties of a few percent reported, for example, to the 2010 XMM Users Group, the 1% threshold used in the analysis is too restrictive and would draw an unnecessarily large amount of attention. The judgement of the RGS IDT is that 2% is a good compromise allowing the following recommendation to be made for the current CCD read-out arrangements:

> For observations of smooth continuum spectra of point sources, in rough terms, any individual RGS CCD with a total count rate in all orders of 12 cts/s in RGS1 and 6 cts/s in RGS2 suffers from pile-up of about 2%.

These limits are used below in conjunction with the wavelength-dependent effective area to draw up the corresponding CCD-dependent flux limits.

5.4.2 Number of pixels affected by RGS pile-up

Fig. 7 shows the number of pixels brighter than the 1% threshold in an individual CCD was very large in some of the brightest sources, implying severe pile-up damage to the spectra. Although the number of pixels affected in Capella is much lower, it does lead to systematic underestimates by a few percent of the fluxes of the brightest lines. Capella is discussed further below in section 7.2.

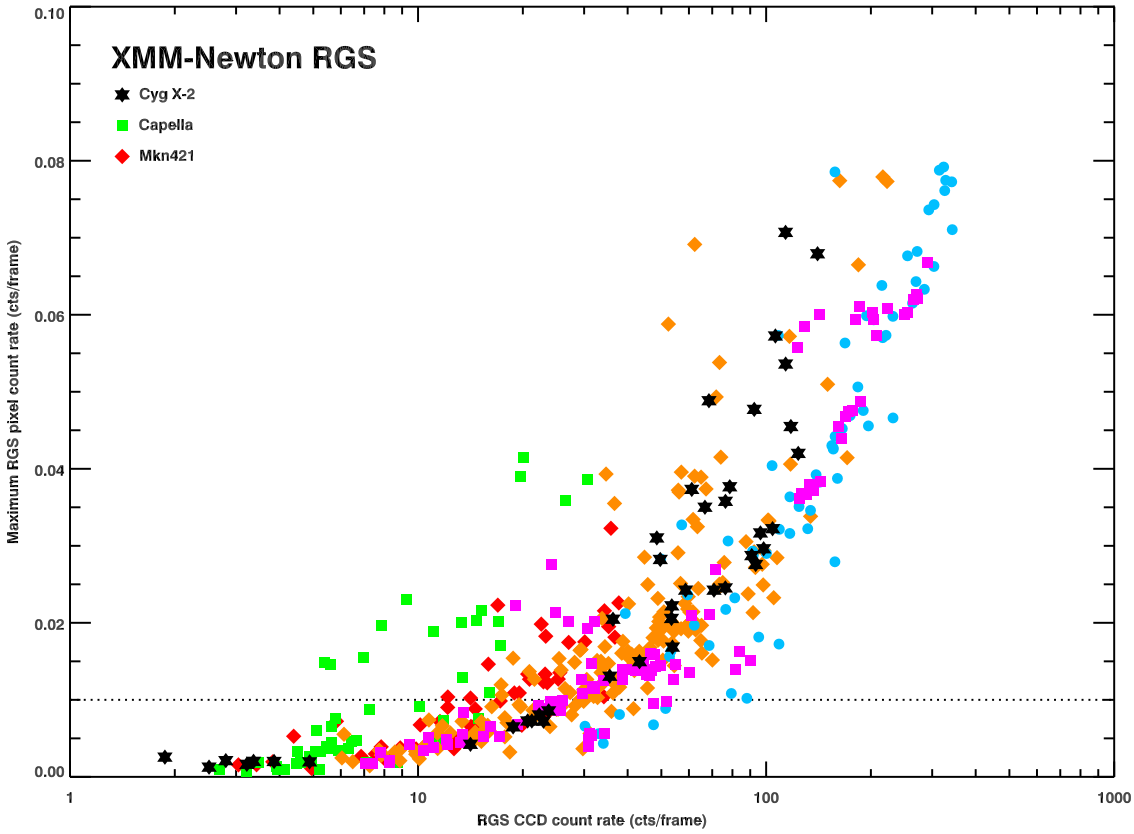

Figure 6: RGS pile-up fraction as a function of CCD count rate. Coloured symbols not shown in the key are for various types of X-ray binary. The black stars below the 1% threshold in the lower left are from the small window mode test on Cyg X-2. Most of the observations of Capella and Mkn421, shown by the red and green symbols, were made for RGS calibration purposes.

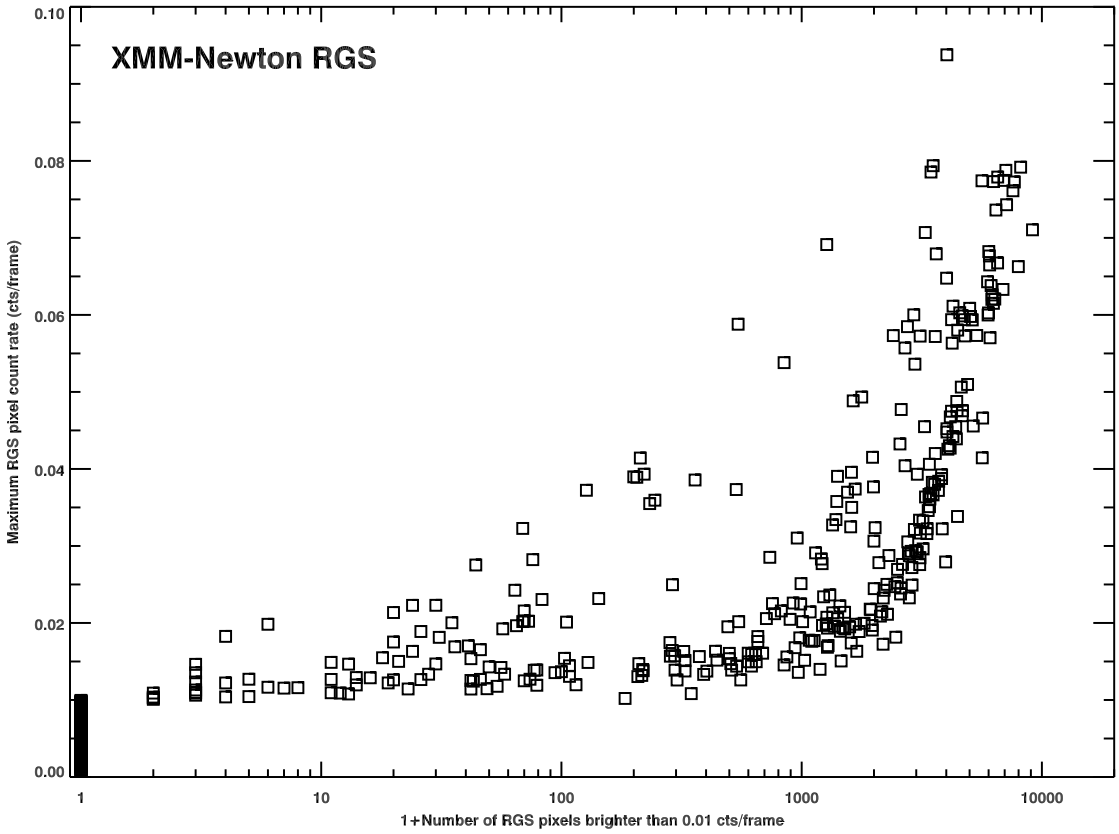

Figure 7: RGS pile-up fraction as a function of the number of CCD pixels brighter than 0.01 counts per frame.

6 Pile-up flux levels for individual RGS CCDs

In section 5.4.1 above, CCD count rate levels of 12 cts/s in RGS1 and 6 cts/s in RGS2 were defined at which the pile-up fraction reaches about 2% in smooth continuum sources. These have been with the observation of the XCal spectra and response matrices of PKS2155-304 in 1734_0411780401 to derive the approximate corresponding physical flux levels on each CCD, as shown below:

		2% pile-up flux (erg cm^{-2} s^{-1})			2% pile-up flux (erg cm^{-2} s^{-1})
RGS1	CCD1	7.1×10^{-10}	RGS2	CCD1	3.1×10^{-10}
RGS1	CCD2	5.0×10^{-10}	RGS2	CCD2	2.1×10^{-10}
RGS1	CCD3	3.8×10^{-10}	RGS2	CCD3	1.6×10^{-10}
RGS1	CCD4	3.3×10^{-10}	RGS2	CCD4	
RGS1	CCD5	2.9×10^{-10}	RGS2	CCD5	1.5×10^{-10}
RGS1	CCD6	3.2×10^{-10}	RGS2	CCD6	1.4×10^{-10}
RGS1	CCD7		RGS2	CCD7	1.9×10^{-10}
RGS1	CCD8	7.1×10^{-10}	RGS2	CCD8	3.7×10^{-10}
RGS1	CCD9	20.0×10^{-10}	RGS2	CCD9	14.1×10^{-10}
double-node readout			single-node readout		

7 Context of the RGS small window mode

7.1 The number of relevant sources

The number of X-ray sources for which RGS pile-up is expected to exceed 2% may be estimated in several ways. The corresponding RASS count rate, which covers nearly the same bandpass as the RGS, is about 20 cts/s. There are 26 RASS catalogue entries brighter than this, including 19 LMXRBs. The brightest 10 sources in descending order were GX339-4, Cyg X-2, Crab, GX9+9, 4U1820-30, GX349+2, HZ43, Ser X-1, 4U1735-44 and Cir X-1, most of which figured in the analysis reported above and were piled-up above the 2% level. Other sources brighter than 20 cts/s in the pointed ROSAT PSPC catalogue include assorted novae, AM Her, LMC X-3, Aql X-1, LQ Hya and AR Lac. A rough estimate from the XMM Slew Survey, which has covered about half the sky so far, adds about another 10 sources. In summary, not forgetting Sco X-1, there are probably between 30 and 50 sources bright enough at any one time to suffer from significant pile-up in the RGS.

7.2 Capella and other active stars

Capella is a bright line-rich X-ray source that shows modest long-term variability of up to a factor-of-two and no obvious flares. It can therefore serve for comparison for observers of other stars. The pile-up fraction in the brightest lines in RGS2 single-node readout is about 5% and about half that value in RGS1. Its mean count rates are about 9 cts/s combining RGS1 and RGS2 1st and 2nd orders; about 100 cts/s in EPIC-pn SW mode; and 24 cts/s in the RASS, where it was the 23rd brightest source. By comparison with Capella, other stars are likely to suffer or have suffered from pile-up. HR 1099 and AB Dor often flare and have been as bright as Capella or brighter during some of these episodes.

7.3 Source Variability

Observers often have some idea of the long-term variability of targets. In objects where historically this has been high but unpredictable, such as Mkn421, PKS2155-304, HR1099, AB Dor and many X-ray binaries, observers might be well-advised to be cautious and choose to use the highest observed states for pile-up estimates should the scientific objective demand it.

7.4 Alternative observing strategies for bright X-ray sources

Astronomers confronting physical questions that take advantage of high-resolution spectra in the RGS band of the 30-50 X-ray sources in the sky have only two realistic alternatives at their disposal, namely *XMM-Newton* and Chandra: Suzaku's low resolution and contamination exclude it from serious consideration. The performance of the RGS small-window test on Cyg X-2 showed that the mode coped well with one of the very brightest sources, so that it is very likely to be suitable for most other bright sources, so there is no obvious need to recommend the use of the Chandra gratings instead. The availability of simultaneous EPIC-pn data offers observers unique opportunities in constraining physical models. The relative calibration of EPIC-pn and RGS in imaging modes has been shown to be of the highest quality and, while there are some particular calibration challenges for the SOC, similar joint efforts promise similar achievements among the brightest sources.

8 Conclusions

The assessment above shows that pile-up is common in RGS observations of bright sources. The science available from XMM would be significantly enhanced if the RGS small window mode could be offered to observers of sources bright enough to require timing modes or other pile-up mitigation methods. It would almost certainly become the mode of choice for most RGS calibration observations of Mkn421 and Capella.

The advantages of the new RGS small window mode in the Cyg X-2 test were clear:

- close correlation between RGS and EPIC-pn variability
- smooth spectra without the damage evident in normal spectroscopy mode

The RGS IDT warmly recommends that the small window mode be offered to the community in AO10.

References

[1] Pileup in RGS spectra, `http://xmm2.esac.esa.int/docs/documents/CAL-TN-0075-1-0.pdf`